



1st International Conference on the Material Point Method, MPM 2017

Interface direct shearing behavior between soil and saw-tooth surfaces by DEM simulation

Xue-Ying Jing^a, Wan-Huan Zhou^{a,b,*}, Yangmin Li^c

^aDepartment of Civil and Environmental Engineering, Faculty of Science and Technology, University of Macau, Macau, China

^bUMacau Research Institute, Zhuhai, Guangdong, China

^cDepartment of Electromechanical Engineering, Faculty of Science and Technology, University of Macau, Macau, China

Abstract

The shearing behavior of a soil-structure interface is influenced by the properties of both the soil and the structure (e.g., particle shape, structural hardness, and surface roughness). While previous investigations using experimental approaches have been able to characterize the macroscopic behavior of the soil–structure interface, the micro-mechanisms behind these observations made from a laboratory still require explanation. This study aims to analyze the effect of roughness on the shearing behavior of the soil-hard structure interface. To do so, we performed a series of three-dimensional interface shear tests using the discrete element method with various degrees of normalized roughness. A standard saw-tooth was chosen to represent the geometry of an artificial rough surface. The results show that: (1) shear stress softening is observed after peak when the specimen shearing is on a rough interface, (2) the shear strength of a soil-structure interface increases as the interface roughness increases, and (3) dilatancy occurs when the roughness is sufficiently large. The incremental shear displacement field indicates that during the shearing process the shear deformation is largely localized in a narrow zone adjacent to the interface, called the shear band. A discontinuous feature is characterized after the shear band appears. The thickness of the shear band varies depending on the roughness of the interface. Specimen shearing on a rougher interface tends to create a thicker shear band.

© 2016 The Authors. Published by Elsevier Ltd.

Peer-review under responsibility of the organizing committee of the 1 st International Conference on the Material Point Method.

Keywords: interface shear test; discrete element method; interface roughness; shear band.

* Corresponding author.

E-mail address: hannahzhou@umac.mo

1. Introduction

The soil-structure interface is found in many geotechnical engineering situations, such as deep foundations, anchor bolts, geogrids for reinforcing soil, etc. The mechanical properties of a soil-structure interface are essential for providing safe and optimal designs within the field of geotechnical engineering. Previous research has revealed that the shearing behavior of the soil-structure interface is influenced by the properties of both the soil and the structure, such as particle shape, grain size distribution, structure hardness, interface roughness, etc. [1,2,3,4]. Previous researchers performed a simple shear test between sand and a steel plate [5] and found that the roughness of the interface and the mean grain size of soil significantly impact the friction coefficient at yield. In another study, a dual interface test was carried out [6] between a granular material and a distinct solid interface. The topography of the interface was determined to affect the frictional resistance, as well as the roughness. The volumetric change in soil induced by interface shearing is also affected by the roughness of the interface [3,7]. These studies suggest that roughness plays a significant role in the macro-mechanical behaviors of soil subjected to interface shearing. Existing research mainly characterizes the macroscopic behavior of a soil–structure interface through laboratory interface shear tests [1, 2, 5, 7, 9]. The macroscopic mechanical behaviors of soil basically originate from the evolution of its fabric, so a better understanding of the macroscopic phenomena of the granular system requires insight into what is happening on the microscopic level.

Taking advantages of the discrete element method (DEM) [10], some numerical interface shear tests have been performed using two-dimensional modeling [11, 12, 13]. Such tests have revealed that the shear strain intensely localizes in a narrow zone, called the shear band. The shear band appears above the structural surface and forms a steady formation in a stable stress state [14]. Once the shear band appears, the soil-structure interface can be considered a region that consists of a thin layer of soil and the interface. In this context, distinguishing the shear band is a premise for further studying the soil-structure interface. Moreover, the reaction of a three-dimensional granular material to interface shearing may differ from a two-dimensional granular material because an additional degree of freedom is included. Therefore, modeling the interface shear test using a three-dimensional method is necessary.

In this study, we performed a series of three-dimensional interface shear tests with distinct degrees of roughness. The input micro-parameters were calibrated according to a real direct shear test under various normal stress conditions to analyze the effects of roughness on the shear strength and the volumetric strain of the soil-structure interface. By doing so, we gained insight into particle behavior and the incremental displacement field of granular assembly under a steady shear stress state. The relationship between the thickness of the shear band and the value of R_n is discussed. These numerical results provide a basic knowledge on the influence of the size of the saw-tooth interface on the mechanical behavior of the soil-structure interface.

2. Numerical modeling

2.1. Model set-up

Fig. 1a illustrates the interface shear test apparatus set-up in PFC 3D (Itasca Consultants, Inc.). The walls constructed in PFC are considered rigid boundaries. The top horizontal wall was vertically moveable to apply a normal force. The bottom rough wall was horizontally moveable to induce interface shearing on the granular material. Around 14000 spherical particles, following a uniform size distribution with a uniformity coefficient C_u of 1.2, were generated within the shear box. The diameters of particles ranged from 0.71 ~ 1.16 times the mean particle diameter d_{50} . To generate a dense specimen, the radius of each particle was gradually increased to fill the shear box. The friction angle of inter-particles remained at zero during the generation process [15]. Although random interface geometries exist in nature, we adopted a standard saw-tooth in this study to represent a rough surface. The front view of the rough surface in the model is shown in Fig. 1b. The inclination of each saw tooth is 45° and 135° alternately, and the horizontal distance between two adjacent valleys is λ . A normalized roughness denoted by R_n [5] was used to qualify the roughness of the interface, which is equal to $\lambda/2d_{50}$ in this case.

In order to mimic the inter-locking phenomenon between authentic soil particles against the rotation (due to the irregularity of particles' shapes), a linear rolling resistance model, which was based on the conventional linear

contact model, was adopted in this study [8, 16, 17]. According to the linear contact rule, the contact force between inter-particles arises linearly from constant normal stiffness k_n , tangential stiffness k_s and the damping coefficient. Furthermore, the internal moment M is incremented linearly as the relative rotation between particles accumulates. This accumulation occurs up to a maximum limiting value M_r , which is defined as:

$$M_r = \mu_r \bar{r} F_n^l \quad (1)$$

where \bar{r} is the effective radius of the contact, F_n^l is the current normal contact force, and μ_r is the rolling resistance coefficient.

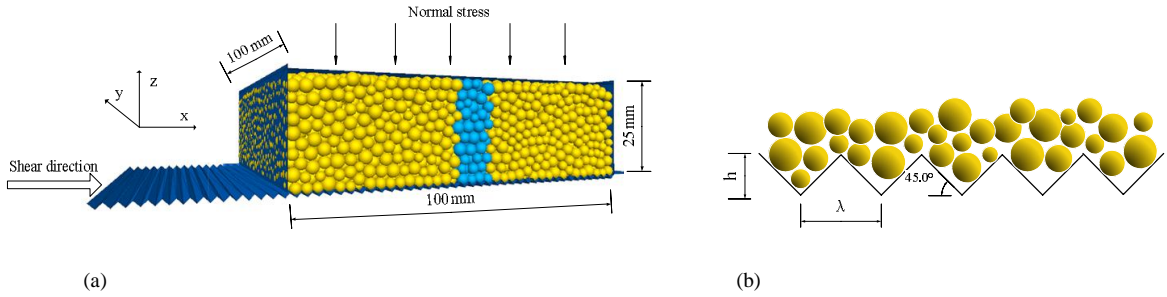


Fig. 1. (a) Schematic diagram of a modified interface shear test; (b) front view of the rough surface.

2.2. Calibration of the input micro-parameters

Table 1. Summary of the input micro-parameters in the DEM model.

Parameters	Value
Model's dimension (m ³)	100×100×25
d_{50} (mm)	3.48
Density (kg/m ³)	2880
Young's modulus (MPa)	50
k_n (N/m)	9×10^9
K ratio (k_n/k_s)	2
Frictional coefficient between particles	0.35
Frictional coefficient between particles and wall	0.2
Rolling resistance coefficient	0.17
Damping coefficient	0.7

The used micro-parameters are summarized in Table 1. We found that the effect of particle mass on the shear strength of granular assembly was slight enough to be negligible, but was significant for computational time [18]. Therefore, twice the density of authentic sand was used in the simulation to enhance the efficiency of calculations. To model a hard structural material, the frictional coefficient between the particles and the wall is 0.2 [12]. The used parameters were calibrated based on a series of direct shear tests on dry completely decomposed granite (CDG) collected from Macau. The initial states of specimens measured in the physical tests and simulations are listed in Table 2. The granular assembly in the simulation followed the same grain size distribution as the physical test. The curves of shear stress versus shear displacement d_s of the DEM simulation and physical tests are compared in Fig. 2. The shear stress measured in the DEM simulation evolved similarly as the value measured in the laboratory tests under various normal stresses. The peak shear stresses measured in the simulation are smaller than the values measured in the physical tests. This may be because the initial specimens were slightly looser than the real CDG

specimen. It should be noted that the shear stress shows a softening after peak in the simulation compared with the real tests. Although the curves of numerical simulations cannot perfectly match the real tests, the simulation can successfully capture the basic mechanical shear behavior of CDG sand. In this context, the input micro-parameters are proven to be reasonable.

Table 2. Initial state of specimens in the physical tests and simulations.

	Dimension of specimen (mm ³)	Particle size (mm)	Normal stress (kPa)	Initial porosity
Physical tests	100 × 100 × 18.5	2.00 ~ 2.36	80/100/120	0.385
Simulations	100 × 100 × 20	1.92 ~ 1.63	80/100/120	0.430

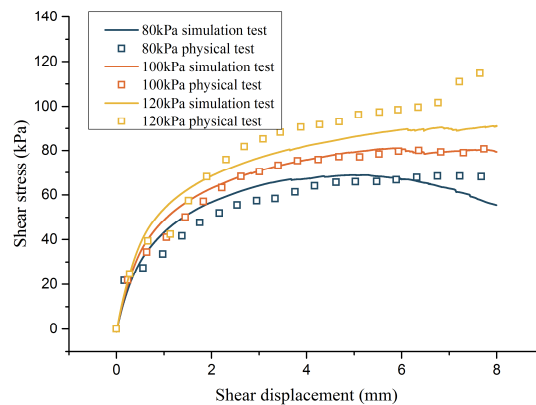


Fig. 2. Shear stress versus shear displacement of simulations and physical tests.

2.3. Simulation process

The granular system had to achieve a state of equilibrium after being created. Then, the top wall was moved vertically to apply a vertical force on the specimen. Next, the bottom plate began to be moved horizontally in the x -direction at a constant rate of 0.015 mm/s. The normal force applied to the top wall is constantly maintained by using a servo system during the shearing process. The macroscopic behaviors of the specimen were obtained from the walls of the shear box, including: (1) the shear stress “ τ ”, which is the shear force measured on the bottom plate divided by the contact area between the soil and the interface, (2) the normal stress “ σ_n ” on the top wall, and (3) the volumetric strain “ ε_v ” obtained from the vertical displacement of the top plate. The maximum shear displacement d_s is 12 mm. A total number of six interface shear tests with various R_n under σ_n of 80 kPa were performed, as shown in Table 3, with an initial porosity of n_0 before shearing.

Table 3. Summary of numerical interface shear tests.

Normalized roughness R_n	Initial porosity n_0
Smooth	0.465
0.1	0.466
0.3	0.461
0.5	0.450
0.7	0.444
1.0	0.432

3. Results and discussion

3.1. Macro-responses of the soil-structure interface with various R_n

The macro-responses of the soil-structure interface are shown in Fig. 3. The stress ratio τ/σ_n increases significantly with the increase of R_n . In cases where the value λ is comparable with d_{50} , namely R_n is close to 0.3, the curves fluctuate strongly after approaching the summit. In these tests, particles overturn from one valley of the surface to the one nearby, which results in this periodic oscillation on the stress ratio τ/σ_n . This kind of periodic oscillation is also observed in the evolution of volumetric strain ε_v . The stress ratio is approximately 0.2 when the shear occurs on a smooth interface, indicating that the τ measured on a smooth interface is mainly attributed to the friction between the bottom soil and the interface material. The peak shear stress ratio increases as the R_n is raised from 0.1 to 0.7. This reinforcement in shear strength of soil is restricted to the threshold value of R_n , which is 0.7 in this study. Furthermore, stress softening occurs when the surface is adequately rough ($R_n \geq 0.3$). In contrast, the interface behaves like an elastic-perfectly plasticity material when the interface is relatively smooth ($R_n \leq 0.1$). The volume of the sample is nearly unchanged when the shear occurs on the smooth interface and dilates when the shear occurs on the rough interface. The motions (up, down, rotation) of particles are triggered when the granular material is sheared on a rough interface. To properly explain these macro-responses of the soil-structure interface, we analyze the particle scale in the following subsection.

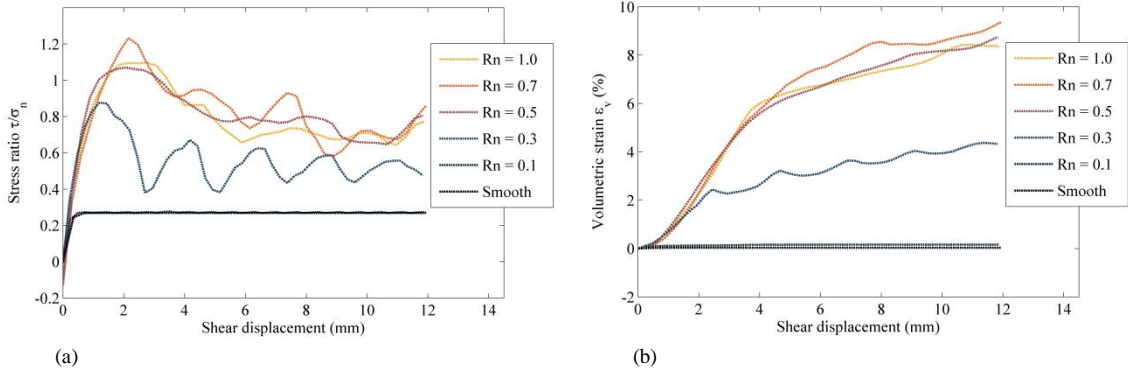


Fig. 3. Macro responses of the soil-structure interface (a) stress ratio (τ/σ_n) versus shear displacement; (b) volumetric strain ε_v versus shear displacement.

3.2. Shear band of interface shear test with various R_n

We obtained the incremental shear displacement field to measure the dimensions of the shear band. The movement of each particle $\vec{u}(x, y, z)$ was monitored at a given stress state. As mentioned in Section 1, the shear band forms a steady formation at a steady stress state. The increment displacement in the x -direction at a steady shear stress ($\delta d_s = 0.2$ mm) is denoted by δu_x :

$$\delta u_x = u_{x1} - u_{x2} \quad (2)$$

where u_{x1} is the u_x of particles at $d_s = 12$ mm, and u_{x2} is the u_x of particles at $d_s = 11.8$ mm. The domain of the material was discretized by constructing a grid. Then, the δu_x of nodes in the grid was interpolated according to the δu_x values of nearby particle centroids using a linear interpolation function. Accordingly, the three-dimensional fields of δu_x can be obtained. As shown in Fig. 4a, the three cross sections A/B/C are set in the shear box. Fig. 4b illustrates the fields of δu_x of the three sections, which are colored according to the δu_x value and shows that a narrow band with intense deformation with an irregular shape appears on the interface. The δu_x field of cross section A, located in the center of the shear box, is chosen to visualize the contour line of the shear band.

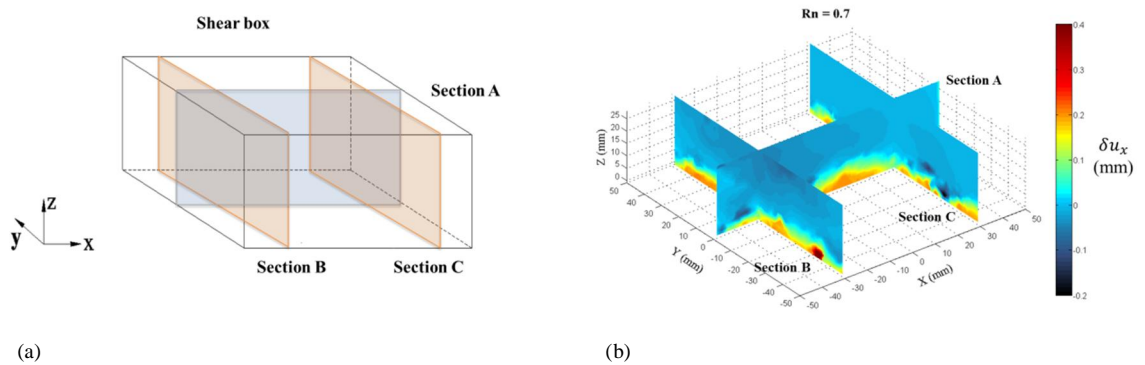


Fig. 4. (a) Location of cross sections A/B/C inside the shear box; (b) incremental displacement fields in the x -direction of sections A/B/C.

The fields of δu_x of cross section A measured in the interface shear tests with various R_n are illustrated in Fig. 5. The area beneath the red dashed line is the shear band area, where the value of δu_x is greater than 0.025 mm ($\delta u_x \setminus \delta d_s \geq 0.125$). The shear deformation is largely localized in the shear band when compared with the upper domain. In contrast, the particles in the upper zone tend to move in the opposite direction of shearing, suggesting that a rougher interface forms a thicker shear band. The interface shear test with R_n of 0.7 generated the thickest shear band, which is about 4 times of d_{50} (measured between the highest point of the shear band and the bottom). Accordingly, a higher peak shear stress is measured on the interface (Fig. 3a). Moreover, the bottom layer of particles is trapped in the valley of the rough interface when R_n is equal to 0.7 or 1.0. These particles moved almost the same displacement as the interface. The granular assembly was organized into two regions after interface shearing. The thickness of the shear band is affected by the value of R_n . Other potentially influencing factors on the thickness of the shear band should be investigated in the future.

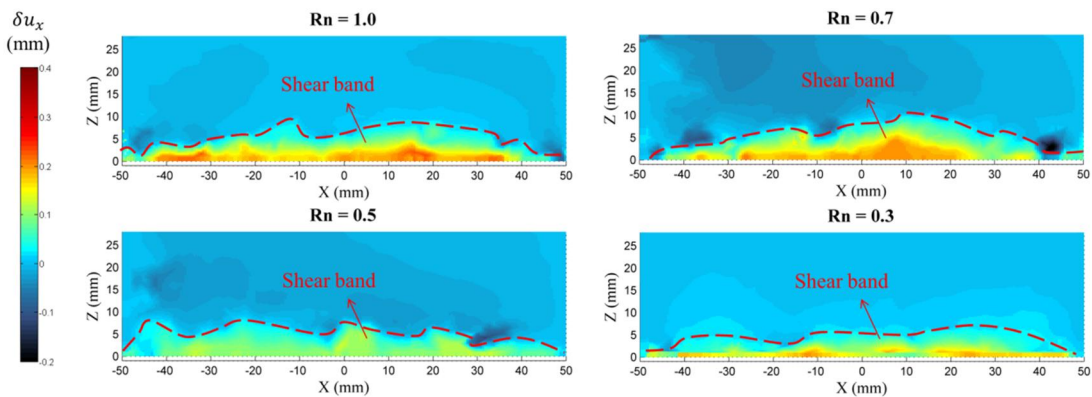


Fig. 5. Incremental displacement fields in the x -direction of the cross section A of interface shear tests with various normalized roughness R_n .

4. Conclusion

In this study, we analyzed the shearing behavior of the soil-structure interface with different saw-tooth interfaces. A series of interface shear tests were performed using three-dimensional DEM simulation. The results show that: (1) stress softening is observed for a rough interface, (2) the shear strength of the soil-structure interface increases with an increasing normalized roughness R_n of the interface, and (3) dilatancy occurs when the R_n is sufficiently large. An analysis on the incremental displacement along the x -direction indicates that shearing deformation is largely localized in a narrow irregular zone (shear band) adjacent to the contact interface during the shearing process. The thickness of the shear band varies with R_n . A rougher interface tends to produce a thicker shear band, and higher

shear strength is measured on the interface. Other influencing factors on the thickness of a shear band remain to be investigated. More evidence is required to confirm the relationship between the thickness of the shear band and the peak shear stress of the soil-structure interface.

Acknowledgements

The authors gratefully acknowledge the financial support from the Macau Science and Technology Development Fund (FDCT) 125/2014/A3 and 011/2013/A1, the National Natural Science Foundation of China (Grant no. 51508585) and the University of Macau Research Funds (Grant nos. MYRG2015-00112-FST and MYRG2014-00175-FST).

References

- [1] M. Uesugi, H. Kishida, and Y. Tsubakihara, "Behavior of sand particles in sand-steel friction," *Soils Found.*, vol. 28, no. 1, pp. 107–118, 1988.
- [2] L. M. Hu and J. L. Pu, "Testing and Modeling of soil-structure Interface," *J. Geotech. Geoenvironmental Eng.*, vol. 130, no. 8, pp. 851–860, 2005.
- [3] J. T. DeJong, D. J. White, and M. F. Randolph, "Microscale observation and modeling of soil-structure interface behavior using particle image," *Soils Found.*, vol. 46, no. 1, pp. 15–28, 2006.
- [4] C. N. Khoury, G. A. Miller, and K. Hatami, "Unsaturated soil-geotextile interface behavior," *Geotext. Geomembranes*, vol. 29, no. 1, pp. 17–28, 2011.
- [5] M. Uesugi and H. Kishida, "Frictional resistance at yield between dry sand and mild steel," *Solids Found.*, vol. 26, no. 4, pp. 139–149, 1986.
- [6] S. G. Paikowsky, C. M. Player, and P. J. Connors, "A dual interface apparatus for testing unrestricted friction of soil along solid surfaces," *ASTM Geotech. Test. J.*, vol. 18, no. 2, pp. 168–193, 1995.
- [7] G. Zhang, D. F. Liang, and J. M. Zhang, "Image analysis measurement of soil particle movement during a soil-structure interface test," *Comput. Geotech.*, vol. 33, no. 4–5, pp. 248–259, 2006.
- [8] C. M. Wensrich and A. Katterfeld, "Rolling friction as a technique for modelling particle shape in DEM," *Powder Technol.*, vol. 217, pp. 409–417, 2012.
- [9] M. A. Hossain and J. H. Yin, "Behavior of a Pressure-Grouted Soil-Cement Interface in Direct Shear Tests.," *Int. J. Geomech.*, vol. 14, no. 1, pp. 101–109, 2014.
- [10] P. A. Cundall and O. D. L. Strack, "A discrete numerical model for granular assemblies," *Géotechnique*, vol. 29, no. 1, pp. 47–65, 1979.
- [11] R. P. Jensen, P. J. Bosscher, M. E. Plesha, and T. B. Edil, "Dem simulation of granular media - structure interface: effects of surface roughness and particle shape," *Int. J. Numer. Anal. Meth. Geomech.*, vol. 23, no. 6, pp. 531–547, 1999.
- [12] J. D. Frost, J. T. Dejong, and M. Recalde, "Shear failure behavior of granular-continuum interfaces," *Eng. Fract. Mech.*, vol. 69, no. 17, pp. 2029–2048, 2002.
- [13] J. F. Wang and M. J. Jiang, "Unified soil behavior of interface shear test and direct shear test under the influence of lower moving boundaries," *Granul. Matter*, vol. 13, no. 5, pp. 631–641, 2011.
- [14] J. F. Wang, S. G. Marte, and E. D. Joseph, "Numerical studies of shear banding in interface shear tests using a new strain calculation method," *Int. J. Numer. Anal. Meth. Geomech.*, vol. 31, pp. 1349–1366, 2007.
- [15] L. Cui and C. O'Sullivan, "Exploring the macro- and micro-scale response of an idealised granular material in the direct shear apparatus," *Géotechnique*, vol. 56, no. 7, pp. 455–468, 2006.
- [16] K. Iwashita and M. Oda, "Rolling Resistance at Contacts in Simulation of Shear Band Development by DEM," *J. Eng. Mech.*, vol. 124, no. 3, pp. 285–292, 1998.
- [17] J. Ai, J. F. Chen, J. M. Rotter, and J. Y. Ooi, "Assessment of rolling resistance models in discrete element simulations," *Powder Technol.*, vol. 206, no. 3, pp. 269–282, 2011.
- [18] T. T. Ng, "Input Parameters of Discrete Element Methods," *J. Eng. Mech.*, vol. 132, no. 7, pp. 723–729, 2006.